

See discussions, stats, and author profiles for this publication at: <http://www.researchgate.net/publication/258323592>

Synthesis of FAU Type Zeolite Y from Natural Raw Materials: Hydrothermal SiO₂-Sinter and Perlite Glass

ARTICLE *in* THE OPEN MINERALOGY JOURNAL · FEBRUARY 2008

DOI: 10.2174/1874456700802010001

CITATIONS

8

READS

8

2 AUTHORS, INCLUDING:



G.E. Christidis

Technical University of Crete

48 PUBLICATIONS 690 CITATIONS

SEE PROFILE

Synthesis of FAU Type Zeolite Y from Natural Raw Materials: Hydrothermal SiO₂-Sinter and Perlite Glass

George E. Christidis* and Hara Papanтони

Technical University of Crete, Department of Mineral Resources Engineering, 73100 Chania, Greece

Abstract: The first synthesis of pure FAU-type zeolite Y from a SiO₂-sinter and perlite glass is presented. FAU-type Zeolite Y was synthesized at 95 ± 2°C after 6-12 hours using gels having SiO₂:Al₂O₃:Na₂O molar ratios of 8.4:1:4.2 and using gels with SiO₂:Al₂O₃:Na₂O molar ratios of 10.5:1:4.2 between 48 and 120 hours reaction time. Except for zeolite Y, zeolite NaP_c, gmelinite-Na and the OH-analogue of sodalite were produced from starting gels with different composition. The cation exchange capacity of zeolite Y was 3.3 meq.g⁻¹ and its specific surface area was 520-550 m².g⁻¹. Most of the specific surface area is allocated to micropores. Zeolite Y synthesized from gels with a SiO₂:Al₂O₃ molar ratio of 10.5:1 has a lattice parameter parameter a₀ = 24.747 Å and a Si/Al ratio 2:1. It is concluded that inexpensive raw materials such as volcanic glasses can be used for the production of high added value zeolite Y.

Key Words: Zeolite Y, volcanic glass, perlite, SiO₂-sinter, synthesis.

INTRODUCTION

Synthetic zeolites can be produced from a variety of natural silica-rich materials including acidic volcanic glasses [1], such as natural and expanded perlite and pumice [2-9]. Although the synthesis of zeolites from volcanic glasses provides the opportunity for upgrading of mineral resources, which are either not exploited or are utilized in other industrial applications, it usually yields zeolitic end products with variable purity [10]. Moreover, in most studies zeolites with small channel diameters are produced, such as zeolite NaP_c and/or the OH-analogue of sodalite, and thus cannot be utilized in the chemical industry. Also the final reaction products contain impurities such as quartz, feldspars and micas (mainly biotite), which do not dissolve during the zeolitization process.

Giordano *et al.* [6] proposed the synthesis of pure zeolite A and X from perlite *via* a two-step reaction process. The first step involved reaction of the glass with NaOH and yielded a solid phase assemblage consisting of zeolite NaP_c ± the OH-analogue of sodalite ± zeolite V depending on the concentration of NaOH, the reaction time and the solid:liquid ratio [6,9], and a Si-rich liquid phase, which reacted with Na-aluminate solutions to form an SiO₂-Al₂O₃-rich gel [6]. The latter was heated at 90-100°C to form pure zeolite A and/or zeolite X according to the composition of the starting gels. Using a similar process, Christidis *et al.* [9] synthesized pure zeolite A and zeolite X from perlite and expanded perlite glasses. In both cases zeolite crystallization from the starting gels was complete.

Although pure FAU-type zeolite X has been synthesized from natural volcanic materials, pure zeolite Y, which is also a FAU-type zeolite, has not been synthesized quantitatively from natural materials yet. Previous attempts to synthesize

zeolite Y yielded reaction products with zeolite Y contents lower than 50% [11-12]. Nevertheless, zeolite Y is easily synthesized from SiO₂-Al₂O₃ gels prepared from pure chemical reagents, with/without addition of seeds and/or organic molecules, which act as templates in the crystallization process ([2,13,14] and references therein).

In this contribution, we present the first quantitative synthesis of pure zeolite Y from SiO₂-rich natural materials such as volcanic glass (perlite) and hydrothermal SiO₂-rich sinters.

MATERIALS AND EXPERIMENTAL METHODS

The SiO₂-rich source materials were provided from S&B Industrial Minerals SA. The perlite comes from the Provatas Perlite Mine, Milos Island, Greece and has been described by Christidis *et al.* [15]. It is a fine-grained material, which resulted during separation of various perlite size fractions by air classification. It is a light coloured rhyolite, with 92% of the grains ranging in size between 20 and 60 µm and 8% between 10 and 20 µm [15]. The perlite consists principally of volcanic glass (>95%), quartz, albite and biotite and has a SiO₂:Al₂O₃ molar ratio of 9.12. It has the following chemical composition [15]: SiO₂ 72.52%, TiO₂ 0.10%, Al₂O₃ 13.39%, Fe₂O₃ 1.41%, MgO 0.57%, CaO 1.15%, Na₂O 3.70%, K₂O 3.41% and LOI 3.21%. The SiO₂-rich sinter is a fine-grained white material (90% < 250 µm) consisting essentially of amorphous SiO₂ (>97%), the remaining being coarse grained quartz (~2%) and traces of amorphous Fe-oxides.

The SiO₂-sinter was dissolved at 95°C, after reaction with a 5N NaOH solution, using a 1:10 solid to liquid ratio for 90 minutes. The perlite was dissolved in an inconel autoclave (Parr Instruments) at 120°C, after reaction with a 2N NaOH solution and a 1:5 solid:liquid ratio for 2 hours. After dissolution the Si-liquid was filtered under vacuum and the Si precipitated in the form of amorphous SiO₂ at pH 8 after neutralization with HCl. The SiO₂ was washed until free of chloride (AgNO₃ test), dried at 105°C and stored. The Na-

*Address correspondence to this author at the Technical University of Crete, Department of Mineral Resources Engineering, 73100 Chania, Greece; E-mail: christid@mred.tuc.gr

aluminate solution was prepared by dissolving suitable amounts of $\text{Al}(\text{OH})_3$ (Merck) in NaOH at 250°C for 60 minutes in an inconel autoclave. The amorphous SiO_2 was mixed with variable volumes of Na-aluminate solution so as to obtain gels with the appropriate $\text{SiO}_2:\text{Al}_2\text{O}_3:\text{Na}_2\text{O}:\text{H}_2\text{O}$ molar ratios.

Two sets of experiments were performed. The first set involved gels with a constant $\text{Na}_2\text{O}:\text{Al}_2\text{O}_3$ molar ratio (4.2:1), and $\text{SiO}_2:\text{Al}_2\text{O}_3$ molar ratios varying from 7:1 to 15:1 and the second set involved gels with a constant $\text{SiO}_2:\text{Al}_2\text{O}_3$ molar ratio (10.5:1) and $\text{Na}_2\text{O}:\text{Al}_2\text{O}_3$ molar ratios varying from 3.2:1 to 5.2:1. The gels were subsequently homogenized for 24 hours at room temperature using continuous stirring (150 rpm). Synthesis of zeolites from the gels was carried out in a teflon-coated spherical reactor at $95 \pm 1^\circ\text{C}$, without stirring. Samples were taken at time intervals of 3-120 hours, washed with deionized water to pH 9 and dried in the atmosphere. All reagents were of analytical grade.

The mineralogy of the reaction products was determined with powder X-ray diffraction (XRD), using a Siemens D500 X-ray diffractometer (CuK α radiation, 35 kV and 35 mA, graphite monochromator). The morphology of the synthetic zeolite crystals was observed on gold-coated powder samples with a JEOL 5400 SEM. Adsorption-desorption isotherms of the zeolites were obtained by N_2 gas adsorption using a NOVA 2200 surface area analyzer (Quantachrome). Samples were degassed overnight at 200°C under vacuum (10^{-2} Torr). Specific surface areas were determined by the BET equation [18] using the P/Po range 0-0.35 of the adsorption branch of the isotherms, while the pore size distribution was determined from the desorption branch of the isotherms. Infrared spectra of zeolite Y were obtained with a Perkin Elmer 1000 FTIR spectrometer. The KBr pellet method was used [17], in the wave number range 400-1200 cm^{-1} in transmission mode, by averaging 25 scans. 1.5 mg of the zeolite was mixed with 200 mg KBr and pressed to 13mm KBr disks, which were subsequently dried at 150°C overnight. The cation exchange capacity (CEC) of the reaction products was determined after saturation with 1N ammonium acetate at pH 7. The samples remained in the acetate solution for 10 days and were washed with methanol to remove excess salt. The acetate solution was replaced every day. The CEC was measured using a Kjeldahl microsteam distillation apparatus and titration with dilute sulphuric acid.

RESULTS

Characterization of the Synthetic Zeolites

The results of the zeolite synthesis from SiO_2 -sinters are shown in (Fig. 1 and 2a). Formation of zeolite Y is favoured from starting gels with $\text{SiO}_2:\text{Al}_2\text{O}_3$ ratios of 8.4:1 and $\text{Na}_2\text{O}:\text{Al}_2\text{O}_3$ ratios of 4.2:1. At these conditions, zeolite Y crystallizes after less than 3 hours, as shown by the appearance of powder diffraction maxima (Fig. 2a). After 6 hours, the starting gel was converted totally to zeolite Y. Longer reaction times yielded trace amounts of zeolite NaP_c and after 12 hours zeolite NaP_c constitutes ca. 5% of the reaction product. The abundance of zeolite NaP_c increases further with longer reaction times. Therefore, it is considered that zeolite NaP_c forms at the expense of zeolite Y.

Similar results were obtained from perlite starting materials (Fig. 1 and 2b). In this case, the abundance of zeolite NaP_c increases further after 47 h. Gels with greater $\text{SiO}_2:\text{Al}_2\text{O}_3$ molar ratios are also suitable for crystallization of zeolite Y. However, crystallization begins after a considerably longer reaction time. For a $\text{SiO}_2:\text{Al}_2\text{O}_3$ ratio of 10.5:1, zeolite Y begins to crystallize after 24 h. Also for a $\text{SiO}_2:\text{Al}_2\text{O}_3$ ratio of 9.5:1 gmelinite-Na is found in the final products. Gmelinite-Na is not stable at higher $\text{SiO}_2:\text{Al}_2\text{O}_3$ ratios. Quantitative formation of zeolite Y is observed after 48h, although minor amounts of amorphous material is also present in these syntheses (see below). Starting gels with $\text{SiO}_2:\text{Al}_2\text{O}_3$ molar ratios greater than 12:1 do not favour crystallization of zeolite Y irrespective of the $\text{Na}_2\text{O}:\text{Al}_2\text{O}_3$ molar ratio.

For $\text{SiO}_2:\text{Al}_2\text{O}_3$ molar ratios lower than 8.4:1 zeolite Y does not form and the OH-analogue of sodalite and zeolite NaP_c are the reaction products (Fig. 1). However, the degree of conversion of the starting gel is limited, since abundant amorphous material is present. Gmelinite-Na and zeolite NaP_c are stable products either at low $\text{Na}_2\text{O}:\text{Al}_2\text{O}_3$ ratios (3.2:1) or at high $\text{Na}_2\text{O}:\text{Al}_2\text{O}_3$ ratios (5.2 :1) and for longer reaction times (Fig. 1B). Zeolite Y is kinetically favoured but reacts to more stable phases with increasing reaction time.

In summary, our results suggest that zeolite Y is stable phase at $\text{SiO}_2:\text{Al}_2\text{O}_3:\text{Na}_2\text{O}$ for molar ratios 8.4:1:4.2 and with reaction times of 6-12 hours or $\text{SiO}_2:\text{Al}_2\text{O}_3:\text{Na}_2\text{O}$ molar ratios 10.5:1:4.2 and reaction times greater than 48h.

The a_0 unit-cell parameter for zeolite Y was calculated from the XRD data using Rietveld refinement. The a_0 obtained for zeolite Y produced from perlite and SiO_2 -sinter with a $\text{SiO}_2:\text{Al}_2\text{O}_3$ ratio of 10.5:1 is $24.747 \pm 0.003 \text{ \AA}$, whereas a_0 measured for zeolite Y synthesized from SiO_2 -sinter with the $\text{SiO}_2:\text{Al}_2\text{O}_3$ ratio of 8.4:1 is larger ($24.813 \pm 0.003 \text{ \AA}$). In both cases, a_0 did not vary with reaction time. The a_0 parameter was used to calculate the Si:Al ratio according to [1]. Hence, zeolite Y produced from both starting materials with a $\text{SiO}_2:\text{Al}_2\text{O}_3$ ratio of 10.5:1 has a Si:Al ratio of 2:1, whereas the zeolite Y produced from the SiO_2 -sinter with $\text{SiO}_2:\text{Al}_2\text{O}_3$ ratio 8.4:1 had a Si:Al ratio of 1.68:1. In both cases these Si:Al ratios are typical for zeolite Y, which displays Si:Al ratios in the range 1.5:1–3:1.

The FTIR powder spectra of zeolite Y produced at different reaction times from both raw materials and starting gels with $\text{SiO}_2:\text{Al}_2\text{O}_3:\text{Na}_2\text{O}$ molar ratio of 8.4:1: 4.2 and from SiO_2 -sinter with $\text{SiO}_2:\text{Al}_2\text{O}_3:\text{Na}_2\text{O}$ molar ratio of 10.5:1:4.2 are shown in Fig. (3). The assignment of the major absorption bands follows [1] and is listed in Table 1. The absorption bands recorded are typical of zeolite Y. The bands at 704 cm^{-1} - 695 cm^{-1} (T-O symmetric stretch) and 573 cm^{-1} - 575 cm^{-1} (double ring), were used to calculate the Al mole fraction in the framework of that zeolite [1].

The band at 577 cm^{-1} (perlite and SiO_2 -sinter with $\text{SiO}_2:\text{Al}_2\text{O}_3$ ratio 10.5:1) and 573 cm^{-1} (SiO_2 -sinter with $\text{SiO}_2:\text{Al}_2\text{O}_3$ ratio 8.4:1) yielded Al mole fractions of 0.26 and 0.27, which correspond to a Si:Al ratio of 2.85:1 and 2.70:1 respectively. The bands at 704 cm^{-1} (perlite and SiO_2 -sinter with $\text{SiO}_2:\text{Al}_2\text{O}_3$ ratio 10.5:1), and 695 cm^{-1} (SiO_2 -sinter with $\text{SiO}_2:\text{Al}_2\text{O}_3$ ratio 8.4:1) yielded Al mole fractions of 0.30 and 0.32 respectively which correspond to Si:Al ratios of 2.33:1

and 2.13:1 respectively. The position of the absorption bands suggests that the zeolite Y synthesized from perlite has a lower tetrahedral Al-occupancy, although the starting gels had identical composition. The reason for the slightly different chemical composition is not fully understood. Moreover the existence of a doublet in the band attributed to symmetric stretch of external linkages of the tetrahedra of the zeolite Y synthesized from SiO₂-sinter (765 cm⁻¹ and 785 cm⁻¹), is indicative of variability of the Si:Al ratio and suggests local heterogeneity of the end products. Nevertheless the a₀ parameter does not vary significantly, because the a₀ measured reflects the overall Si:Al ratio in these samples. Also it should be noted that the Si:Al ratios obtained from FTIR data are larger than their counterparts calculated from XRD data. Since calculation of a₀ using Rietveld refinement is reliable, the XRD method is considered more accurate for calculation of the Si:Al ratio than IR spectroscopy.

pure zeolite Y is 520-550 m².g⁻¹, whereas end products containing other zeolites have smaller SSA. The use of t-plots,

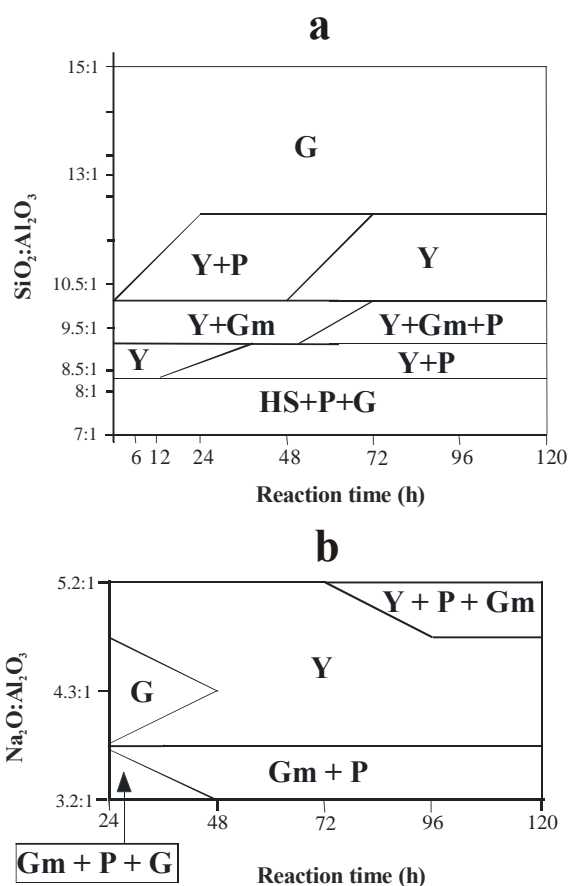


Fig. (1). Crystallization fields of the synthetic zeolites formed in the system: a) SiO₂:Al₂O₃-time plot for a Na₂O:Al₂O₃ molar ratio of 4.2:1 and b) Na₂O:Al₂O₃-time plot for a SiO₂:Al₂O₃ molar ratio of 10.5:1. Y= zeolite Y, P=zeolite NaP_c, Gm=gmelinite-Na, HS=the OH-analogue of sodalite, G=amorphous material.

The cation exchange capacity (CEC) of the synthetic zeolite products varies between 3.3 and 3.6 meq.g⁻¹ and the BET specific surface area varies between 410 and 550 m².g⁻¹. The CEC of pure zeolite Y is 3.30 meq.g⁻¹. The end products containing gmelinite-Na in addition to zeolite Y have higher CEC, in accordance with the lower Si:Al ratio of gmelinite-Na [16]. The BET specific surface area (SSA) of

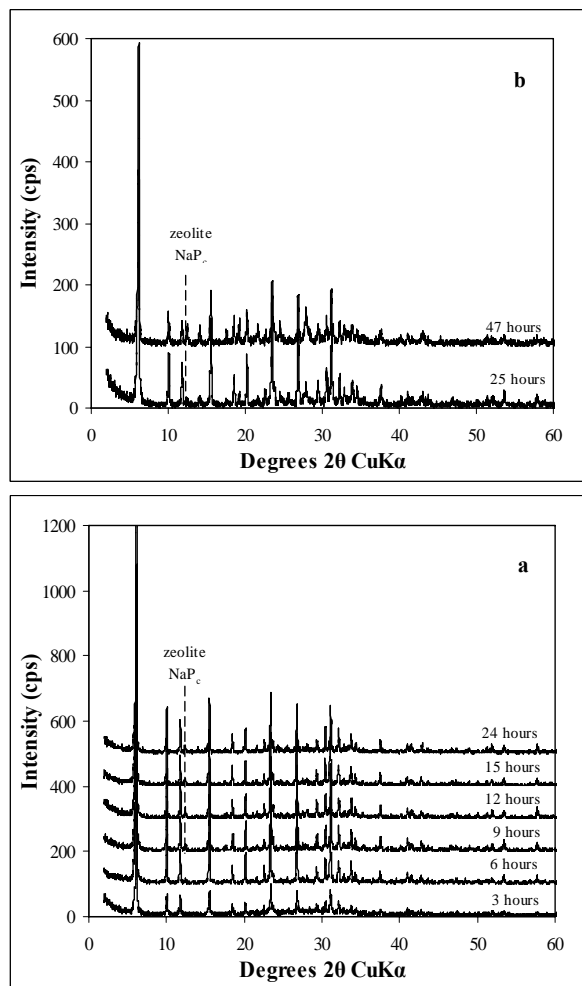


Fig. (2). XRD diagrams showing zeolite Y synthesized a) from SiO₂-rich sinters and b) from perlite.

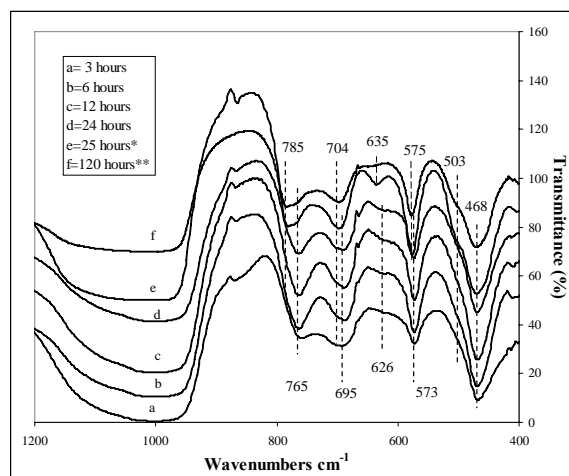


Fig. (3). FTIR spectra of synthetic zeolite Y, a-d= from SiO₂-sinter and SiO₂:Al₂O₃ ratio 8.4:1, e= from perlite and SiO₂:Al₂O₃ ratio 8.4:1, f= from SiO₂-sinter at SiO₂:Al₂O₃ ratio 10.5:1.

Table 1. Assignment of IR Lattice Vibration Bands (Wavenumbers [cm^{-1}]) for Zeolite Y from SiO_2 -Sinters and Perlite (after [1])

Assignment of Bands	Type of Vibration	Zeolite Y (Sinters)	Zeolite Y (Perlite)
Internal tetrahedral	T-O SS	695,703*	704
	T-O bend	468,500,503*	468, 503
External vibrations of tetrahedral linkages	Double ring	573, 577*, 626, 638*	578, 635
	SS	765, 785*	785
	AS	1100	1100

*= $\text{SiO}_2:\text{Al}_2\text{O}_3$ Ratio 10.5:1, Rest Zeolites 8.4:1. SS= Symmetric Bond Stretching, AS= Asymmetric Bond Stretching.

which plot the volume of gas adsorbed versus the statistical thickness of an adsorbed gas film (t) and which are used for quantitative evaluation of microporosity [19], showed that in all end products most of the specific surface area available to N_2 gas is allocated to micropores. Also the N_2 -adsorption isotherms are type-I isotherms (Langmuir-type isotherms), typical of microporous materials [19] (Fig. 4). No hysteresis was observed in the N_2 -desorption branches. Those end products containing gmelinite-Na adsorbed lower volumes of N_2 gas, in accordance with the SSA results. Application of the Langmuir equation allowed an estimation of the SSA, assuming that meso- and/or micropores are essentially absent. The SSA values obtained are higher than the BET SSA (data not shown).

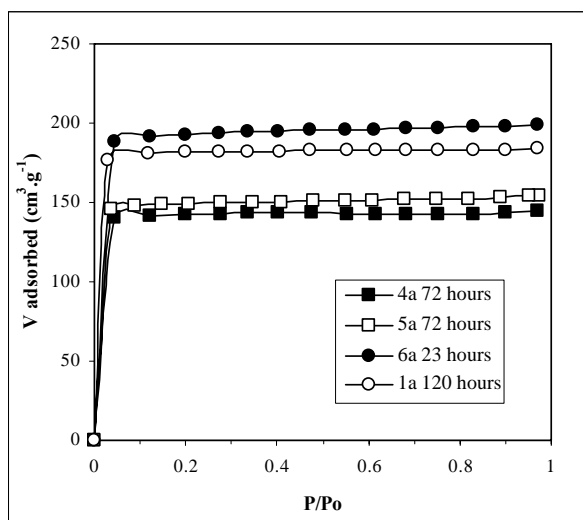


Fig. (4). Adsorption isotherms of the synthetic zeolites. 1a, 4a, 5a, 6a= $\text{SiO}_2:\text{Al}_2\text{O}_3:\text{Na}_2\text{O}$ molar ratios of starting gel. 1a = 10.5:1:4, 4a= 10.5:1:5, 5a=9.5:1:4, 6a=8.4:1:4.

Morphological Features of the Zeolite Y Crystals

The morphology of zeolite Y crystals produced from the SiO_2 -sinter at different reaction times, using starting gels with $\text{SiO}_2:\text{Al}_2\text{O}_3:\text{Na}_2\text{O}$ molar ratios 10.5:1:4.2 is shown in the micrographs in Fig. (5). At 48 h reaction time there is amorphous material which has not crystallized to zeolite Y (arrows in Fig. 5a). The crystal size of zeolite Y is 1-1.5 μm . With increasing reaction time the remaining starting gel crystallizes out to zeolite Y and the crystal size tends to increase. After 72 h reaction time crystal size is ca. 2 μm becoming 3 μm after 120 h. However in both the 72 h and the

97 h reaction products two generations of crystals are visible: larger crystals 2- 2.5 μm in size and smaller crystals ca. 1 μm in size. At 120 h the crystal size is more uniform. Frequently the zeolite crystals form aggregates several tens of microns in size. Zeolite crystals form in general cubes with rounded edges. Octahedral crystals are often present (arrows in Fig. 5b) and twinning is also common (arrow in Fig. 5c). There is evidence that crystal growth proceeds with formation of spirals after nucleation. Spiral growth is better observed in long term experiments, because crystal size is large enough for observation (arrows in Fig. 5d).

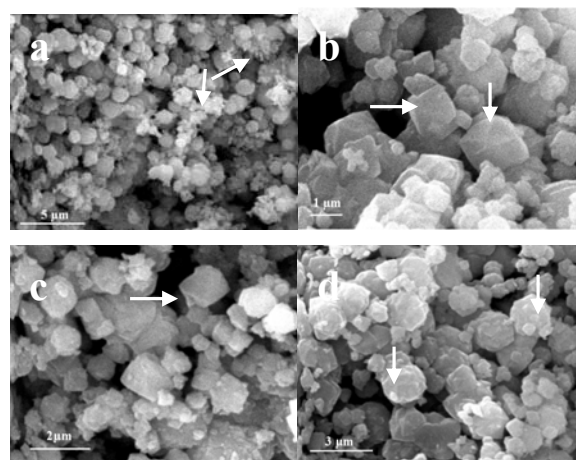


Fig. (5). SEM micrographs of zeolite Y end products produced from SiO_2 -sinter. a) 48 h reaction time. The arrows indicate amorphous matter. b) 72 h reaction time. The arrows indicate crystals with octahedral habit. c) 97 h reaction time. The arrow indicates zeolite Y twins. d) 120 h reaction time. The arrows indicate the formation of growth spirals on the surface of zeolite Y

DISCUSSION

This work has shown that both the SiO_2 -sinter and perlite glass can be utilized as raw materials for synthesis of pure FAU type zeolite Y. Under the experimental setup used zeolite Y can be formed after 6-12 hours. Longer reaction times yield small amounts of zeolite NaP_c . However the abundance of the latter zeolite is small so as to consider that even these experiments yield zeolite Y quantitatively. Compared with previous experiments which yielded other zeolite species, this setup involves complete separation of amorphous SiO_2 from the original volcanic glass, because the form of amorphous SiO_2 is important for synthesis of zeolite Y. Hence the Si-O linkages in volcanic glasses seem to be unfavourable for the nucleation of zeolite Y and so is the $\text{SiO}_2\text{-Al}_2\text{O}_3$ gel

produced from polymerization of the Si-rich solution from the dissolution of volcanic glass [6,9]. In the latter case it is considered that the experimental setup cannot produce starting gels with appropriate $\text{SiO}_2:\text{Al}_2\text{O}_3:\text{Na}_2\text{O}:\text{H}_2\text{O}$ molar ratios for crystallization of zeolite Y, due to experimental constraints. Therefore zeolite A and/or zeolite X form instead of zeolite Y. Note that the perlite used is unsuitable for direct synthesis of zeolite Y although it has a $\text{SiO}_2:\text{Al}_2\text{O}_3$ molar ratio of 9.12 [8], which is comparable to that necessary for synthesis of zeolite Y. Direct dissolution of perlite yields zeolite P_c, zeolite V and the OH-analogue of sodalite [8]. In contrast the amorphous SiO_2 produced from the SiO_2 -sinter and perlite favours synthesis of zeolite Y. It is considered that the onset of crystallization of zeolite Y occurs at considerably shorter time than 3 hours because at that time the zeolite yield exceeded 60% (Fig. 2a).

According to the FTIR spectra and the SEM micrographs the zeolite Y crystals synthesized from the SiO_2 -sinter are inhomogeneous in two aspects: a) the Si:Al ratio of the crystals and therefore their cation exchange capacity and b) zeolite crystal size. With respect to their Si:Al ratio an Al poorer and an Al-richer variety have been recognized in the FTIR spectra. The possibility for an inhomogeneous starting gel is rejected because all gels were homogenized during aging *via* continuous stirring. In an attempt to explain the compositional heterogeneity the filtrate solutions after crystallization of representative zeolite products were analyzed for Si and Al. The $\text{SiO}_2:\text{Al}_2\text{O}_3$ ratio of the solutions does not remain constant with time, but increases dramatically with increasing reaction time (Fig. 6), suggesting that zeolite Y may become progressively enriched in Si. Since nucleation of new crystals from the starting gel occurs simultaneously with crystal growth for at least 48 h (Fig. 5a) it follows that the younger smaller crystals might be richer in Si, and that part of this Si will be included in the growing crystals. Crystal growth proceeds with spiral growth, *via* dissolution of previously formed, unstable crystals, which are richer

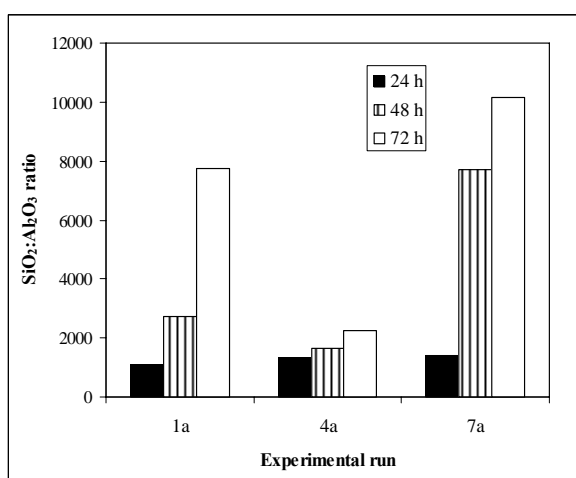


Fig. (6). Evolution of the $\text{SiO}_2:\text{Al}_2\text{O}_3$ molar ratio in the fluid phase of the starting gel during crystallization of zeolite Y from SiO_2 -sinter at various experimental runs. 1a, 4a, 7a= $\text{SiO}_2:\text{Al}_2\text{O}_3:\text{Na}_2\text{O}$ molar ratios of starting gel. 1a=10.5:1:4, 4a=10.5:1:5, 7a=10.5:1:3.

in Al than their younger smaller counterparts formed at a later stage. This Al will counterbalance, at least partially, the excess Si. In this sense the observed compositional inhomogeneity of zeolite Y can be explained at a local scale, although the overall Si/Al ratio does not change significantly during synthesis as is indicated by the a_0 parameter. The final Si/Al ratio of zeolite Y is controlled by the availability of Si.

The fact that the first zeolite Y to form is relatively richer in Al may explain the formation of less siliceous zeolites such as zeolite NaP_c and gmelinite-Na at longer reaction times. With increasing crystallization time the gel becomes progressively richer in Si compared to Al (Fig. 6) and the original Al-richer zeolite crystals are expected to be unstable and dissolve, forming Al-richer domains. In such domains the Si:Al ratios may be suitable to form Al-richer zeolites. As expected, the composition of the starting gel also affects the composition of zeolite Y. Hence the zeolite Y synthesized from the SiO_2 -sinter and starting gels with $\text{SiO}_2:\text{Al}_2\text{O}_3$ ratio 10.5:1 have a larger Si:Al ratio as is indicated both by the a_0 values and the FTIR spectra (spectrum f in Fig. 3). However, these zeolites contain Si-richer and Si-poorer domains as is indicated by the existence of the doublets at 765 and 785 cm^{-1} in the FTIR spectra (Fig. 3), the formation of which was explained previously.

REFERENCES

- [1] Breck, D.W. *Zeolite molecular sieves*; J. Wiley & Sons, N.Y., **1974**.
- [2] Barrer, R.M. *Hydrothermal chemistry of zeolites*; Academic press, London, **1982**.
- [3] Burriesci, N.; Crisafulli, M.L.; Saija, L.M.; Pollizotti, G. *Mater. Lett.*, **1983**, 2, 74.
- [4] Burriesci, N.; Crisafulli, M.L.; Giordano, N.; Bart, J.C.J.; Pollizotti, G. *Zeolites*, **1984**, 4, 384.
- [5] Antonucci, P.L.; Crisafulli, M.L.; Giordano, N.; Burriesci, N.; *Mater. Lett.*, **1985**, 3, 302.
- [6] Giordano, N.; Recupero, V.; Pino, L.; Bart, J.C.J. *Ind. Miner.*, **1987** 83.
- [7] Barth-Wirsching, U.; Höller, H.; Klammer, D.; Konrad, B. *Mineral. Petrol.*, **1993**, 48, 275.
- [8] Christidis, G.; Paspaliaris, I.; Kontopoulos, A.; *Appl. Clay Sci.*, **1999**, 15, 305.
- [9] Christidis, G.; Galani, K.; Marcopoulos Th. In: *Industrial Minerals and Extractive Industry Geology*, Scott, P.W.; Bristow C.M. Eds. Geological Society, London, **2003**; pp. 345-350.
- [10] Breck, D.W. *Industrial Minerals and Rocks*; Lefond S. J. Ed. Transactions AIME, **1983**, pp. 1399-1413.
- [11] Yoshida A.; Inoue K. *Zeolites*, **1986**, 6, 467.
- [12] Aiello, R.; Colella, C.; Sersale R. *ACS Monogr.*, **1971**, 101, 51.
- [13] Coker E.N.; Jansen J.C. *Molecular Sieves Science and Technology*; Karge H.G.; Weitkamp J. Eds.; Springer, Berlin, **1998**, pp. 121-155.
- [14] Guth J-L.; Kessler H. J. *Catalysis and zeolites, fundamentals and applications*; Weitkamp and L. Puppe Eds.; Springer, Berlin, **1999**; pp. 1-52.
- [15] Christidis, G.; Paspaliaris, I.; Kontopoulos, A. *Quar. Rev. Mining Geotech. Metal. Eng.*, **1996**, 6, 63
- [16] Brunauer, S.; Emmet, P.H.; Teller, E. *J. Am. Chem. Soc.*, **1938** 60, 309.
- [17] Russell J.D. *A handbook of determinative methods in clay mineralogy*; Wilson M.J. Ed., Blackie, Glasgow & London, **1987**; pp. 133-173.
- [18] Gottardi, G.; Galli E. *Natural zeolites*; Springer Verlag, Berlin, **1985**.
- [19] Sing, K.S.W.; Everett, D.H.; Haul, R.A.W.; Moscou, L.; Pierotti, R.A.; Rouquerol, J.; Siemieniowska, T. *Pure Appl. Chem.*, **1985**, 57, 603.